APPARATUS FOR MEASURING EMITTANCE AND ABSORPTANCE AND RESULTS FOR SELECTED MATERIALS

by Henry B. Curtis and Ted W. Nyland

Lewis Research Center
Cleveland, Ohio

APPARATUS FOR MEASURING EMITTANCE AND ABSORPTANCE

AND RESULTS FOR SELECTED MATERIALS

By Henry B. Curtis and Ted W. Nyland

Lewis Research Center
Cleveland, Ohio

NATIONAL AERONAUTICS AND SPACE ADMINISTRATION

APPARATUS FOR MEASURING EMITTANCE AND ABSORPTANCE
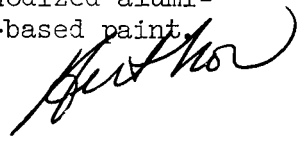
AND RESULTS FOR SELECTED MATERIALS

by Henry B. Curtis and Ted W. Nyland

Lewis Research Center

SUMMARY

13826

An apparatus for measuring hemispherical total emittance and normal solar absorptance is described. A steady-state heat balance method is used in making measurements at specimen temperatures between 280° and 600° K. A carbon-arc solar simulator that is used in the absorptance measurements is described. A description of a blackbody normal absorptance standard is given. Results are given for the following surfaces: four plasma-sprayed ceramics, zirconium silicate, strontium titanate, calcuim titanate, and barium titanate; two ceramics applied by the Rokide process, Rokide MA and Rokide ZS; anodized aluminum, uncoated and electrophoretically blackened; and a white epoxy-based paint. The accuracy of the apparatus is discussed.

INTRODUCTION

The prediction and control of temperature in space systems is dependent on a knowledge of the thermal radiation parameters of the materials used on the surfaces viewing the space environment. Two of the important radiation parameters are hemispherical total emittance and normal solar absorptance. The relative importance of these parameters depends on the temperature level and the space environment. For example, in a space power system, the size of a radiator with a required heat-rejection rate and a given temperature distribution is a function of the hemispherical total emittance. The effect on radiator size and weight due to variable thermal properties such as hemispherical total emittance is further discussed in reference 1. As the operating temperatures of space systems or components assume lower levels (under 600° K), the solar absorptance of the surfaces must also be considered. An example of this situation is a satellite with negligible internal heat generation. Such a satellite would achieve an equilibrium temperature dependent on the hemispherical total emittance, solar absorptance, and thermal environment during operation.

Many problems involving coatings for space systems have been encountered in projects undertaken at the Lewis Research Center. This report describes an ap-

paratus that is used to measure hemispherical total emittance and normal solar absorptance (hereinafter referred to as emittance and absorptance, respectively).

A unique feature in the operation of the apparatus is the capability of making emittance and absorptance measurements on the same test specimen under simulated space conditions of vacuum and temperature. This is a direct measurement of the radiation parameters used in heat-transfer analyses of space systems. The apparatus operates on a steady-state energy balance principle and was designed and assembled at the Lewis Research Center. Similar calorimetric measurement techniques are described in references 2 to 7.

Measurements of emittance and absorptance on a variety of selected materials are included in this report. These radiation parameters are given for such coatings as plasma-sprayed ceramics and epoxy-based paint.

The ultimate uses of these coatings include low-temperature radiators (under 600° K), which require a high emittance, and temperature control surfaces of space systems and experiments.

SYMBOLS

A	area of test surface, sq cm
A_O	area of receiver, sq cm
E	voltage across heater plate heating element, v
F	fraction of specimen radiation incident on receiver
F_O	fraction of receiver radiation incident on specimen
$f(Q_O)$	power absorbed by test surface from receiver, w
$f(Q_S)$	power absorbed by test surface from solar simulator, w
H	intensity of simulated solar irradiance, w/sq cm
I	current through heater plate heating element, amp
P	power dissipated in heater plate without solar irradiance, w
P'	power dissipated in heater plate with solar irradiance, w
Q	power emitted from test surface, w
Q_I	power internally dissipated in heater, w
Q_L	extraneous power exchange, w
Q_O	power emitted from receiver surface, w

$\dot{Q}_S$ simulated solar power, w

T specimen temperature, $^{\circ}K$

T_O receiver temperature, $^{\circ}K$

α hemispherical absorptance of specimen for receiver radiation

α_S normal solar absorptance of specimen

ϵ hemispherical total emittance of specimen

ϵ_O hemispherical total emittance of receiver

σ Stefan-Boltzmann constant, $w/(sq\ cm)(^{\circ}K^4)$

MEASURING TECHNIQUE

A steady-state energy-balance method is used in making measurements of the radiation parameters. A schematic diagram of the test apparatus is shown in figure 1. The test specimen is attached to a heater plate that contains a
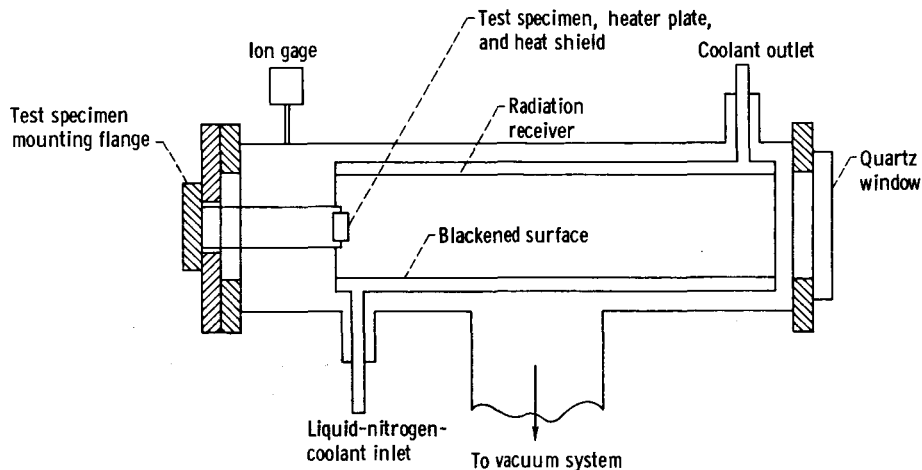

Figure 1. - Schematic of test apparatus.

source of internal heat. This assembly is placed in a known thermal environment and is isolated in such a manner that the only form of heat transfer from the assembly is by radiation from the test surface. With a test specimen of known area, the temperature of the test specimen assembly is measured along with the power required to maintain that temperature. With these data the emittance is calculated from the following equation, which was derived from an energy balance and the Stefan-Boltzmann law:

$$\epsilon = \frac{P}{\sigma A(T^4 - T_O^4)} \tag{1}$$

A derivation of this equation is given in appendix A.

The absorptance is determined by measuring the power required to maintain the test specimen assembly at the same temperature under two conditions: with and without simulated solar irradiance incident normally to the test specimen.

The difference in the two power measurements is the rate at which simulated solar energy is being absorbed. This technique is a modification of the procedure used in measuring solar irradiance with an angstrom pyrheliometer (ref. 8). If the solar irradiance H is known, the absorptance can be calculated from the following equation:

$$\alpha_S = \frac{P - P'}{AH} \qquad (2)$$

TEST APPARATUS

The test facility is designed to measure the emittance and the absorptance and includes the following apparatus:

(1) An evacuated blackbody low-temperature radiation receiver

(2) A test specimen assembly

(3) A support or mounting assembly that minimizes external energy losses from the specimen

(4) A carbon-arc solar simulator

(5) Two automatic temperature controllers

Test Specimen

The test apparatus is designed to use square samples 6.45 square centimeters (1 sq in.) in surface area. The sample is applied or bonded to an aluminum substrate (fig. 2). Aluminum is normally used as the substrate material because of its high thermal conductivity. The test sample and the substrate are hereinafter referred to as the test specimen. A 32-gage (0.008-in.-diam.) iron-constantan thermocouple is peened into the edge of the test specimen for temperature measurements.
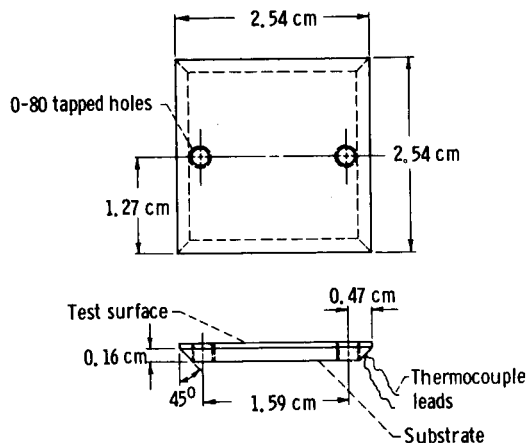
Test Chamber

A schematic diagram of the test apparatus can be seen in figure 1. The test chamber consists of a stainless steel cylinder 63 centimeters long and 20 centimeters in diameter. The radiation receiver is located concentrically within the chamber and consists of a hollow sleeve 55 centimeters long with an inside diameter of 15 centimeters. Liquid nitrogen is circulated through the sleeve to maintain the receiver at a known low temperature. The interior surface of the receiver is blackened with carbon black to obtain a high absorptance

Figure 2. - Test specimen.

.surface. A quartz window clamped on one end flange of the test chamber admits simulated solar radiation. The test specimen and the mounting assembly are supported from the opposite end flange and are positioned so that the plane of the test specimen is perpendicular to the longitudinal axis of the cylinder. A vacuum system, which consists of a liquid-nitrogen-baffled oil diffusion pump, evacuates the test chamber to the range of 10^{-7} torr.

Test Specimen Mounting Assembly

A cutaway drawing of the test specimen mounting assembly is shown in figure 3. The test specimen is held with two cap screws to a heater plate. At times, a thin layer of vacuum grease is spread between the test specimen and the heater plate to ensure good thermal contact. No differences in measured radiation parameters of the test specimen due to the presence of the grease have been noted. The heater plate is made from aluminum 2.4 centimeters square by 3 millimeters thick. A series of grooves is milled part way through the plate, and a length of 36-gage (0.005-in.-diam.) fiber-glass-insulated Chromel wire is cemented into each groove. This wire is the resistive heating element within the test spe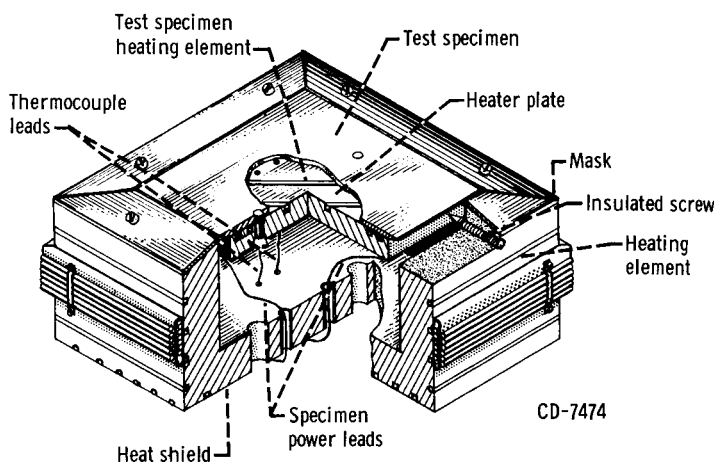cimen assembly. A 36-gage iron-constantan thermocouple is peened into the surface of the plate and is used as the sensing element in a temperature control system.

Figure 3. - Test specimen assembly and heat shield.

The test specimen and the heater plate together are known as the test specimen assembly. The test specimen assembly is centered inside a temperature-controlled heat shield with four thermally insulated screws as shown in figure 3. The heat shield is made of aluminum in the form of a square cup having inside dimensions of 2.7 by 2.7 by 1.4 centimeters. Thirty-two-gage fiber-glass-insulated-iron wire is cemented in a series of grooves milled on the outside surface and is used as the heating element for the heat shield. A 36-gage iron-constantan thermocouple is attached to the shield and used as the sensing element of a second temperature control system. Both the test specimen assembly and the heat shield are controlled to the same temperatures by two automatic controllers, which are described in the following section.

For the purpose of reducing radiant heat losses from the edge of the test specimen, a mask is placed on the outside surface of the heat shield and is adjusted so that the slot width between the test specimen surface and the heat shield is minimized. The power and potential leads from the test specimen as-
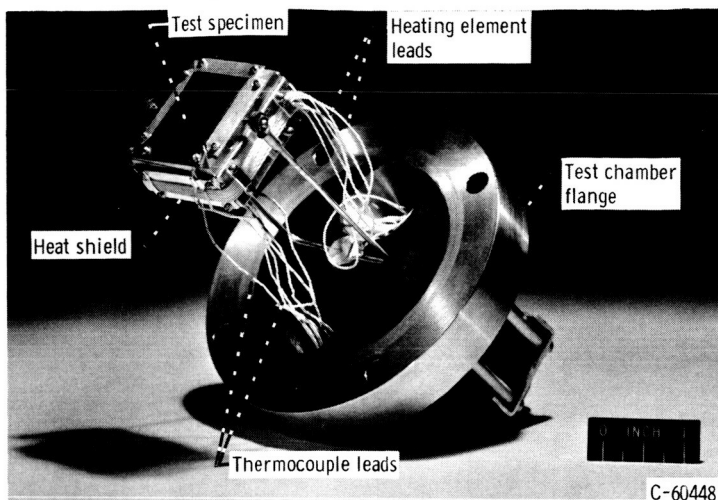
Figure 4. - Test specimen mounting assembly with flange.

sembly and the heat shield are wrapped around the heat shield so that a negligible amount of power from the test specimen is lost because of thermal conduction.

The test specimen can be mounted to the heater plate without removing the heater plate from the cup assembly. The cap screws are inserted through two holes in the heat shield and into the test specimen. In this manner the need for making a heater element for each test specimen is eliminated. The entire test specimen mounting assembly is supported from an end flange and is shown in figure 4.

Automatic Temperature Controllers

A block diagram of the temperature measurement and the control systems is shown in figure 5. The purpose of the control systems is to maintain the test specimen assembly and the heat shield at the same temperature so that any heat transfer between these two elements is made negligible. For control, a null-balance method is employed that uses two similar control systems for the heat shield and the test specimen assembly.

In both systems, the electromotive force of the thermocouple used for temperature measurement and control is referenced to a cold junction and compared with a known set-point voltage. The difference between these voltages is an error signal that is detected by a commercial null meter. The set-point voltage is stabilized with a temperature-compensated Zener diode. A transistorized power amplifer, similar to that described in reference 9, is placed across the indicator circuit of the null meter. The output of the power amplifier is a current that is a function of the thermocouple-set-point error signal. This current flows through the
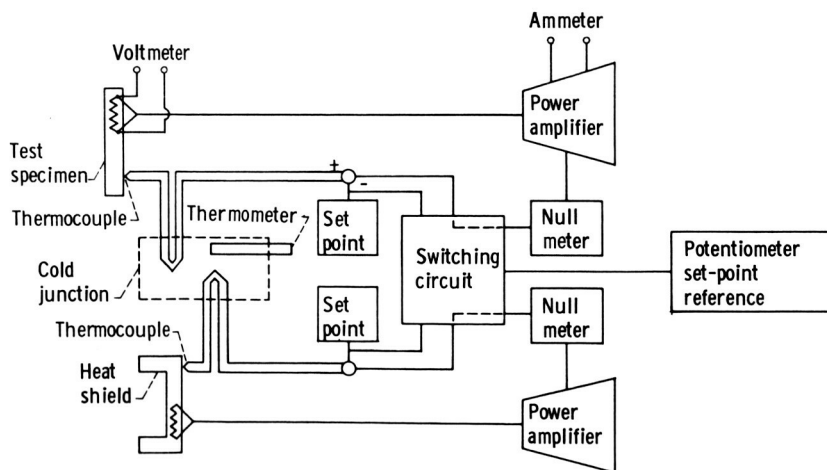

Figure 5. - Temperature control system.

heating element and thus controls the temperature.

The power generated within the test specimen assembly is determined by measuring the voltage drop across and the current through the heater element. A commercial potentiometer is used in making these power measurements. A switching circuit provides a means for measuring the temperature set-point voltage externally with a potentiometer and for balancing the heat shield set point against the test specimen assembly set point.
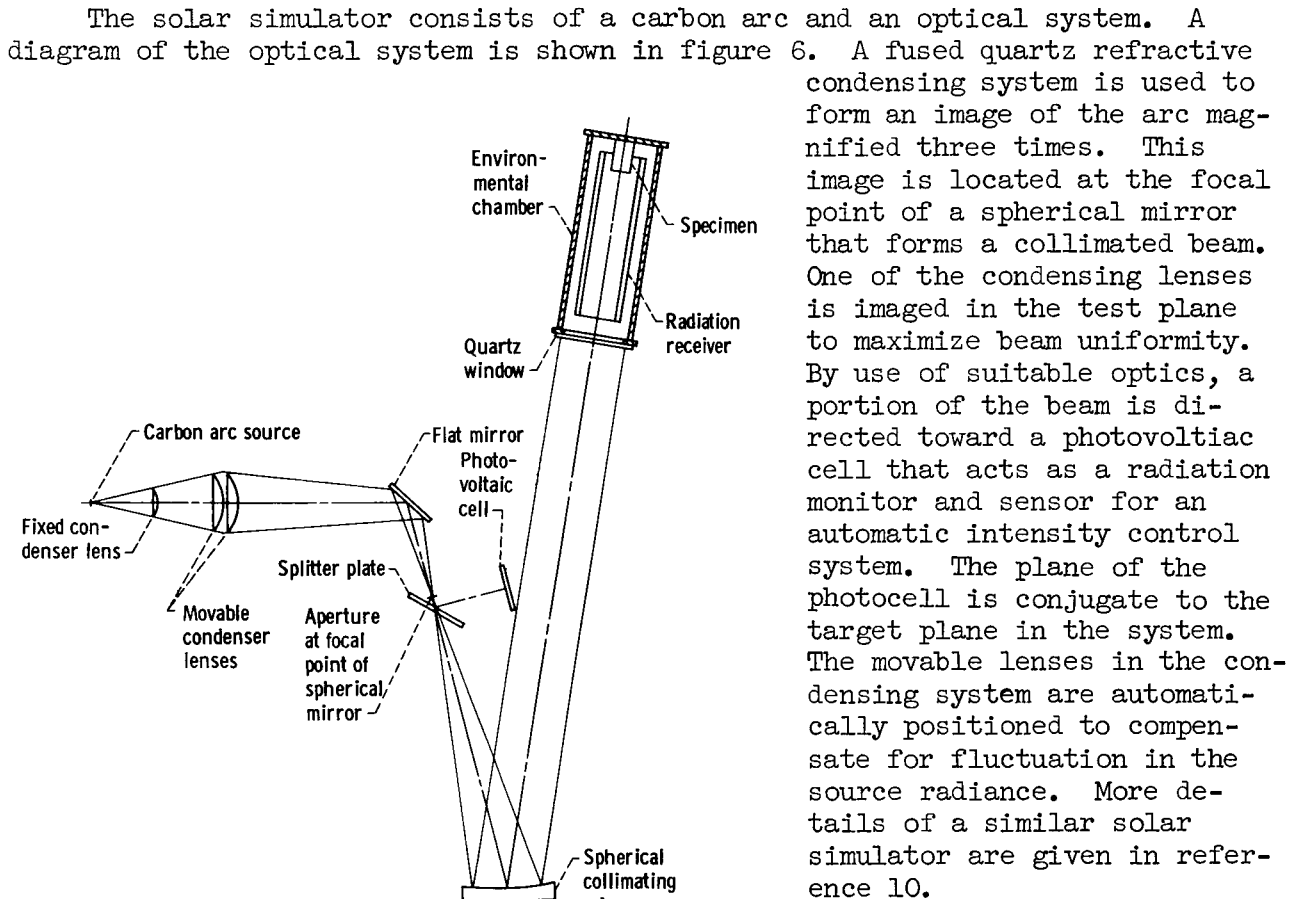
Solar Simulator

The solar simulator consists of a carbon arc and an optical system. A diagram of the optical system is shown in figure 6. A fused quartz refractive condensing system is used to form an image of the arc magnified three times. This image is located at the focal point of a spherical mirror that forms a collimated beam. One of the condensing lenses is imaged in the test plane to maximize beam uniformity. By use of suitable optics, a portion of the beam is directed toward a photovoltiac cell that acts as a radiation monitor and sensor for an automatic intensity control system. The plane of the photocell is conjugate to the target plane in the system. The movable lenses in the condensing system are automatically positioned to compensate for fluctuation in the source radiance. More details of a similar solar simulator are given in reference 10.

Figure 6. - Diagram of optical system of solar simulator.

The output of the simulator is a collimated beam with a flux density equal to that of solar radiation outside the atmosphere of the Earth (0.14 w/sq cm ±2 percent). The spectral distribution of the irradiance of the simulator has been measured, and the best known values are plotted in figure 7. Numerous difficulties are encountered in measuring such spectral distributions; hence, there is considerable uncertainty about this curve. For comparison, a normalized Johnson curve, which is the generally accepted spectral distribution of solar energy outside the atmosphere of the Earth (ref. 11), is also shown in figure 7. The areas under both curves have been made equal.
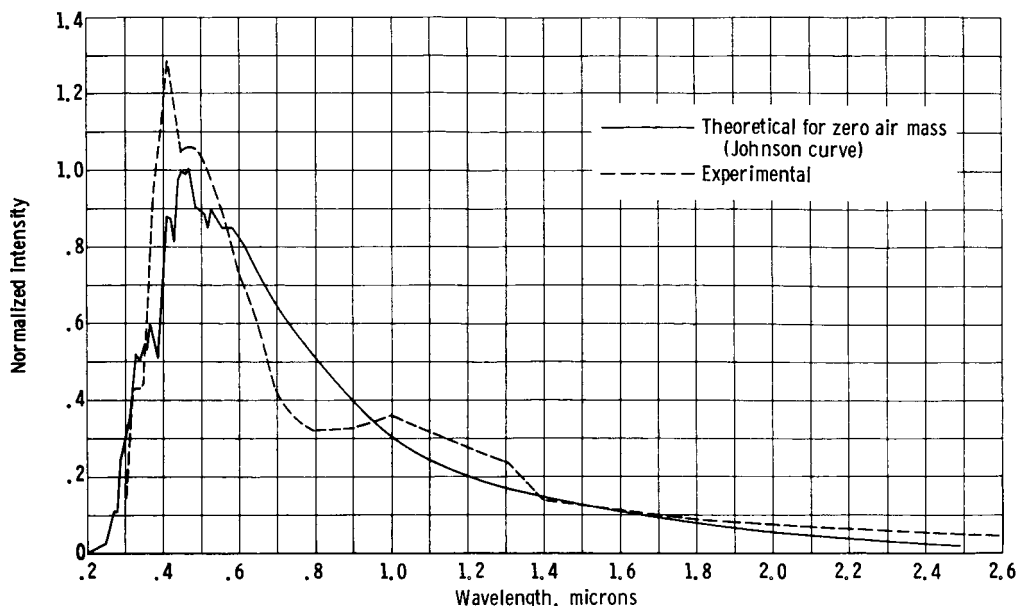
Figure 7. - Normalized spectral distribution of solar simulator irradiance.

Calibration of the total irradiance of the simulator is described in appendix B.

APPARATUS ACCURACY

Emittance Measurements

A comprehensive error analysis has been performed to determine instrument accuracy. A similar error analysis of the calorimetric techniques for measuring emittance is given in reference 12. This analysis, along with some experimental verification, indicates that emittance measurements are accurate to ±5 percent of the readings over the range of measurements cited in this report. The instrument is inherently more accurate at higher temperatures, and the emittance measurement is within ±2 percent at 600° K. The following list indicates the main sources of error and their magnitudes for the instrument and measurement technique:

(1) Temperature measurement (±1° K)

(2) Power measurement (0.3 percent)

(3) Assumption of black body radiation receiver (<±0.1 percent)

(4) Heat losses due to nonisolation of test specimen assembly (±3 percent)

    (a) Thermal conduction in lead wires

    (b) Extraneous radiation exchange from test specimen assembly

    (c) Residual gas conduction

(d) Thermal conduction through mounting arrangement

(5) Assumption of gray body test surface (±0.4 percent)

(6) Nonequilibrium of specimen temperature during measurement (±1 percent)

The major portion of uncertainty in the measurements is associated with the heat-loss term. The magnitude of the heat-loss term depends on the design and the operation of the apparatus. The emittance measurements have been repeatable to within ±1 percent. This indicates that random errors in the measurements are negligible to this degree.

Absorptance Measurements

The sources of error inherent in the absorptance measurement are divided into those associated with the solar simulator and those associated with the rest of the test apparatus. The error due to the solar simulator is mainly caused by the mismatch between the spectral distribution of irradiance of the simulator and the Johnson curve and the uncertainty in such measurements. It should be emphasized that the magnitude of error depends on the spectral absorptance of a particular test surface. Such an error would occur if the spectral absorptance of a test surface were high in a wavelength band where the simulator had an excess of output irradiance. In that case, more energy would be absorbed by the test surface than under true solar irradiance. This might lead to an error in the measured absorptance of 20 to 30 percent.

Since the power is measured under two identical thermal conditions, many of the errors associated with the test apparatus are effectively cancelled, as indicated in the section Emittance Measurements. However, a major portion of the error in the absorptance measurement is caused by not having identical thermal equilibrium conditions during the two power measurements. Also, uncontrolled fluctuations in the total irradiance of the solar simulator cause additional error in absorptance measurements. The magnitude of error not involved with the spectral distribution of the solar simulator is estimated to be ±5 percent. Repeatability tests have shown that most of this error is random in nature.

RESULTS

Ceramic Coatings

Measurements of emittance and absorptance have been made on several ceramic coatings applied to aluminum substrates. These coatings are being investigated for possible use on radiators operating under 600° K. The ceramic coatings that were measured are barium titanate, calcium titanate, Rokide MA, Rokide ZS, strontium titanate, and zirconium silicate. Figure 8 shows emittance as a function of temperature for six ceramics. The coating mass per unit area, determined by weighing the specimen before and after application of the coating, is given as well as the approximate thickness, which may be in error by ±0.02 millimeter. Table I gives the emittance at 500° K for each specimen.
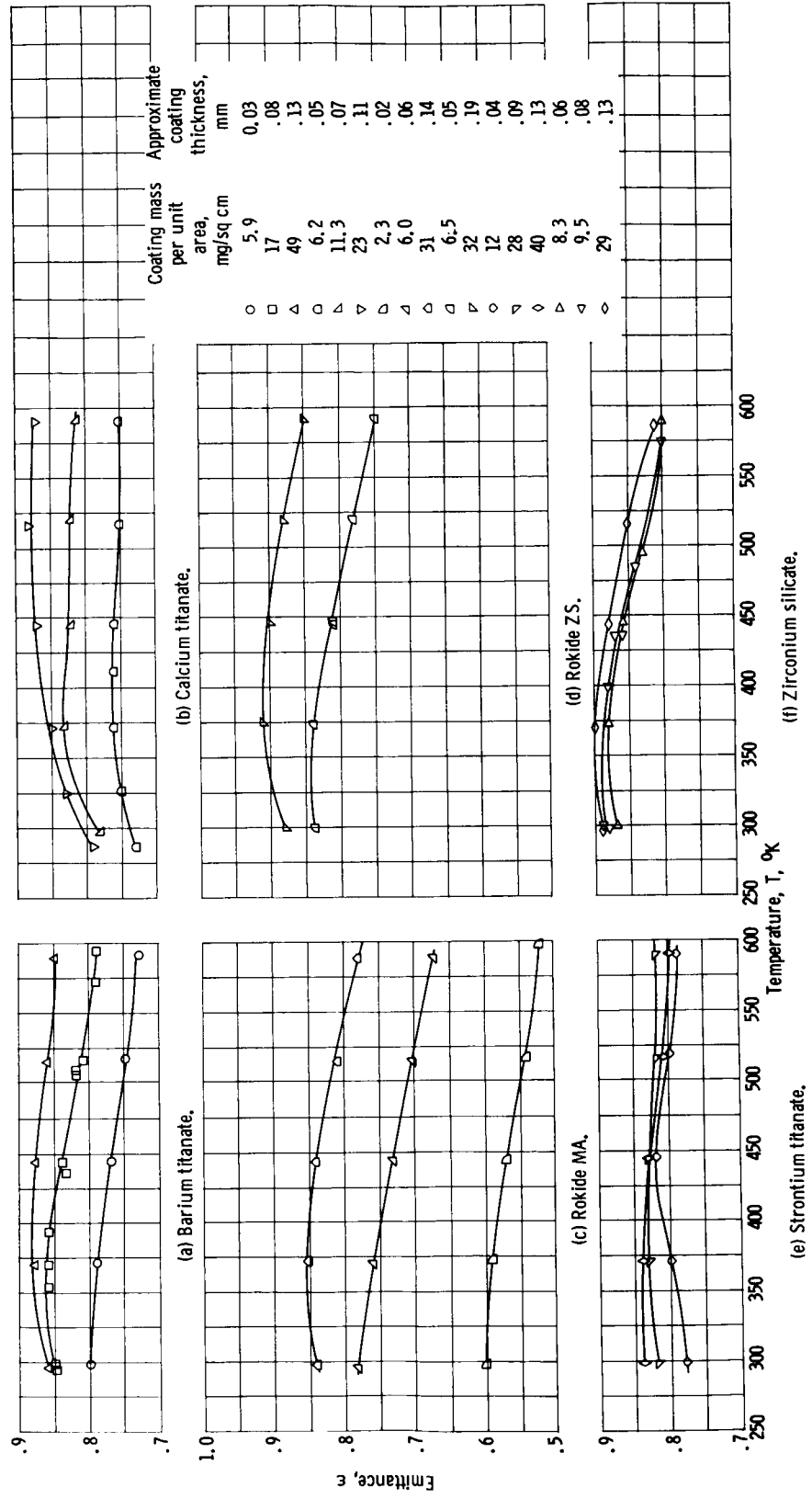
Figure 8. - Emittance of ceramic coatings as function of temperature.

10

TABLE I. - EMITTANCE AND ABSORPTANCE

FOR CERAMIC COATINGS

Coating	Coating mass per unit area, mg/sq cm^2	Emittance,[a] ϵ	Absorptance,[b] α
Barium titanate	5.9 17 49	0.75 .82 .87	0.65 .61 .74
Calcium titanate	6.2 11.3 23	0.75 .82 .88	0.72 .70 .70
Rokide MA	2.3 6.0 31	0.55 .71 .82	0.55 .58 .41
Rokide ZS	6.5 32	0.79 .89	0.54 .45
Strontium titanate	12 28 40	0.81 .82 .83	0.73 .76 .64
Zirconium silicate	8.3 9.5 29	0.83 .83 .86	0.46 .38 .37

[a]At 500° K.
[b]At 400° K.

Table II gives results of X-ray diffraction tests and spectrographic analyses for the constituents of the test specimens.

There is little dependence of emittance on temperature; however, there is an increase in emittance as coating mass increases. This can be seen in figure 9, in which emittance at 500° K is plotted against coating mass. For any of these specific coatings, increasing the coating mass up to approximately 15 milligrams per square centimeter increases the emittance of the coating. Beyond 15 milligrams per square centimeter, there is little further change in emittance. Comparison of the emittance values with those published in reference 13 shows a general agreement in the overlapping temperature region.

The absorptance data of each specimen are given in table I. In general, the absorptance is constant with tem-

TABLE II. - X-RAY DIFFRACTION AND SPECTROGRAPHIC

ANALYSIS OF CERAMIC COATINGS

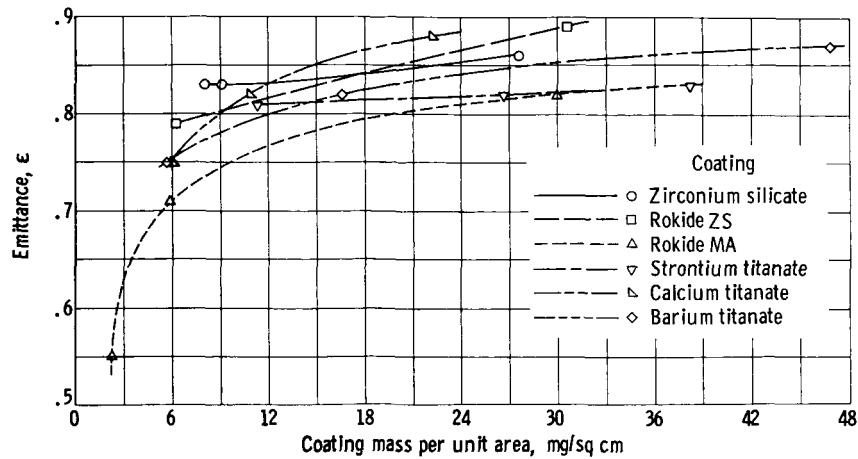| Coating	X-ray diffraction analysis	Spectrographic analysis
Barium titanate	$BaO \cdot TiO_2$	Ba - Ti - Al - Si, Cu
Calcium titanate	$CaO \cdot TiO_2$ (perovskite)	Ti, Ca - Zr, Mg, Al - Na, B, Cu, Si, Fe, Ni, Pb, Mn
Rokide MA	$MgO \cdot Al_2O_3$	Al, Mg - Si - Fe, B, Ti, Na, Mn, Ga
Rokide ZS	ZrO_2 (cubic)	Zr, Si - Al - Mg, Ca - Ti, Cu, B, Fe
Strontium titanate	$SrO \cdot TiO_2$	Sr, Ti - Al, Fe, Ca, Si, Cu, Pb
Zirconium silicate	ZrO_2 (cubic)	Zr, Si - Hf, Al, Ti, Fe, Cu, Ta

Figure 9. - Coating-mass increase at 500° K.

perature over the measured range of 400° to 600° K. Two of the coatings, calcium and barium titanate, however, showed a marked drop in absorptance of approximately 0.1 during the first heating to 600° K. After the initial heating, these specimens exhibited no further change in absorptance. This change is always a drop in absorptance, never an increase. The reason for this change is unresolved. The final stabilized absorptance values are given in table I. Table III denotes the general appearance of the specimens before and after testing. All specimens had a mat finish.

Anodized Aluminum

Measurements of emittance and absorptance were made on four anodized aluminum specimens. Two of the specimens had a layer of carbon electrophoretically deposited into the pores of the anodized aluminum. Two other anodized specimens were left uncoated. The purpose of the carbon black coating is to obtain a lightweight, high emittance coating. It was desired to determine the increase in emittance caused by adding the carbon layer to the anodized aluminum specimens.

TABLE III. - DESCRIPTION OF CERAMIC COATINGS

Coating	Method of application	Appearance	
		Before test	After test
Barium titanate	Plasma-arc spraying	Dark gray	No change
Calcium titanate	Plasma-arc spraying	Gray with red tint	Gray
Rokide MA	Rokide process	Gray with blue tint	No change
Rokide ZS	Rokide process	Light gray with blue tint	No change
Strontium titanate	Plasma-arc spraying	Dark gray	No change
Zirconium titanate	Plasma-arc spraying	Light gray	No change

The emittance measurements were made in the temperature range 300° to 600° K. Plots of emittance as a function of temperature for two uncoated anodized specimens (1 and 2) are given in figure 10. Since specimen 1 was duller in appearance than specimen 2, there was probably a thickness variation that could account for the difference in emittance between the two. The emittance data for the two blackened specimens (3 and 4) are also given in figure 10. These two specimens were similar
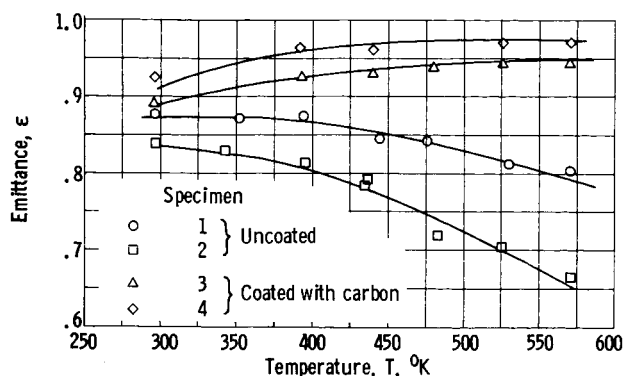
12

Figure 10. - Emittance of plain and black anodized aluminum as function of temperature.

in appearance and were black in color.

The addition of the carbon layer has a definite effect on emittance. The two uncoated specimens both exhibited decreasing emittance with temperature, while the black specimens exhibited slightly increasing emittance with increasing temperature. The difference in emittance between uncoated and blackened specimens at 600° K is approximately 25 percent with the black specimens at 0.95. A summary of data for the anodized specimens is presented in table IV. The absorptance values are constant over the measured temperature range. A large increase in absorptance occurs because of the addition of the carbon.

Tile Coat Paint

Measurements of emittance and absorptance have been made on aluminum substrates coated with Tile Coat, (manufactured by Wilbur & Williams, Norwood, Mass.) a white epoxy-based paint with a titanium dioxide pigment. Measurements were made on two specimens at 320° K. In order to apply the paint to one specimen, the substrate was dipped into the paint, and the excess was allowed to drain off. This resulted in a smooth even coating. The paint was sprayed on the other substrate and appeared whiter. The thicknesses of the paint coatings were both about 0.2 millimeter. The data for the two specimens are given in table IV.

TABLE IV. - EMITTANCE AND ABSORPTANCE OF ANODIZED

ALUMINUM AND WHITE EPOXY-BASED PAINT

Coating	Emittance, ϵ	Temperature during emittance measurement, $^{\circ}$K	Absorptance, α	Temperature during absorptance measurement, $^{\circ}$K
None (anodized) specimen 1)	0.83	500	0.57	400 to 600
None (anodized specimen 2)	.71	500	.48	400 to 600
Carbon black (anodized specimen 3)	.94	500	.97	400 to 600
Carbon black (anodized specimen 4)	.97	500	.97	400 to 600
Dipped tile coat	.89	320	.38	320
Sprayed tile coat	.89	320	.34	320

The emittance is consistent and agrees with previous results published in reference 11. From table IV it is seen that the method of application and handling affects the absorptance values. The sprayed coating had an absorptance that was 11 percent lower than the dipped coating; this difference was also visually apparent. The absorptance data reported herein are much higher than that in reference 14 (0.20). Part of this difference can be attributed to spectral mismatch between the solar simulator used in the measurements reported herein and the Johnson curve.

An attempt was made to estimate the error in absorptance readings due to this spectral mismatch. An analysis using the spectral absorptance of the Tile Coat paint given in reference 14 and the spectral distribution of the solar simulator given in figure 7 indicates that the absorptance readings reported herein are 15 percent high. The remaining discrepancy must be attributed to the uncertainty in the measured spectral irradiance of the simulator or to a similar uncertainty encountered by the investigators of reference 14.

CONCLUDING REMARKS

An apparatus has been developed for measuring the emittance and the absorptance of a wide variety of surfaces in the temperature range 280° to 600° K. Emittance measurements were made in the range 0.52 to 0.97, and absorptance measurements covered the range from 0.34 to 0.97. Overall accuracy of the emittance measurements was estimated to be within ±5 percent. The absorptance measurements are considered accurate to ±5 percent of those for a perfect solar simulator. Since the spectral distribution of the irradiance of the simulator does not match the Sun's irradiance exactly, an additional absorptance error is involved, depending on the spectral absorptance of the specimen. Repeatability of measurements for a given specimen has been ±1 percent for emittance and ±5 percent for absorptance.

In general, where comparisons are available, the measured emittance data agree with published results. There is a large difference, however, between measured and published absorptance data for Tile Coat paint, which are the only absorptance data compared. This seems to indicate that, if any appreciable error is inherent in the measurements reported herein, it is in the irradiance of the solar simulator or in the techniques of applying and handling the coatings.

From emittance measurements of various ceramic coatings it was found that there is a coating thickness beyond which application of additional ceramic has little effect on emittance. It was also noted that the emittance did not vary much with temperature for the ceramic coatings.

Lewis Research Center
    National Aeronautics and Space Administration
        Cleveland, Ohio, October 8, 1964

DERIVATION OF EQUATIONS

The expressions for determining emittance and absorptance are derived by applying an energy balance to the test specimen assembly. Consider a test specimen attached to a heater plate, as shown in figure 11.
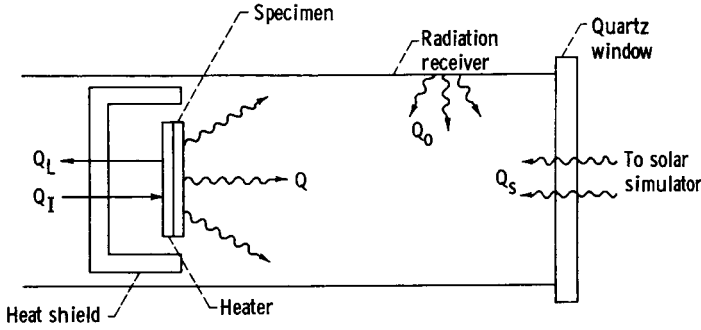

Figure 11. - Test specimen attached to heater plate.

The test specimen assembly is enclosed in a radiation receiver with nonreflecting walls. It is assumed all radiation emitted by the test surface is incident on the radiation receiver. In figure 11, Q is the power emitted from the test surface, Q_O is the power emitted from the radiation receiver surface, Q_S is simulated solar power, Q_I is the power internally dissipated in the heater, and Q_L is any other extraneous power exchange.

In the test apparatus, the test specimen and the heater plate are enclosed in a heat shield, so that there is no radiant heat exchange between the back and sides of the test specimen assembly and the radiation receiver. Thus, an energy or power balance applied to the test specimen assembly is as follows:

$$f(Q_O) + f(Q_S) + Q_I = Q + Q_L \tag{A1}$$

The expressions $f(Q_O)$ and $f(Q_S)$ are the amounts of power absorbed by the test specimen surface from the radiation receiver and the solar simulator, respectively. The terms in equation (A1) can be rewritten by means of the Stefan-Boltzmann law and other heat-transfer considerations and expressed in terms of measurable parameter, including the absorptance and emittance:

$$f(Q_O) = \sigma A_O \epsilon_O T_O^4 F_O \alpha \tag{A2}$$

$$f(Q_S) = \alpha_S A H \tag{A3}$$

$$Q_I = EI = P \tag{A4}$$

$$Q = \sigma A \epsilon T^4 \tag{A5}$$

The apparatus was designed to minimize Q_L, and it is assumed equal to zero. The Q_L term includes conduction and convection from the test specimen assembly and radiation exchange between the sides of the test specimen assembly and the radiation receiver. Also, since the test is made at steady-state temperature conditions, there is no change in stored energy within the test speci-

men assembly.

Equation (A2) is simplified by making two assumptions:

(1) The radiation receiver acts as a black diffuse body. Therefore

$$\epsilon_O = 1$$

and

$$A_O F_O = AF = A$$

since $F = 1$.

(2) The specimen acts as a gray body. Therefore

$$\epsilon = \alpha$$

Hence

$$f(Q_O) = \sigma A \epsilon T_O^4 \qquad (A6)$$

When emittance is measured, no solar irradiance is incident on the specimen ($H = 0$); hence, equation (A1) reduces to

$$\sigma A \epsilon T_O^4 + P = \sigma A \epsilon T^4 \qquad (A7)$$

$$\epsilon = \frac{P}{\sigma A (T^4 - T_O^4)} \qquad (A8)$$

To measure absorptance, the specimen is exposed to simulated solar irradiance of intensity H. The term Q_I is adjusted to a new value P' so as to maintain the specimen temperature at the value it had during the emittance test.

Therefore, equation (A1) reduces to

$$\sigma A \epsilon T_O^4 + \alpha_S AH + P' = \sigma A \epsilon T^4 \qquad (A9)$$

Since the temperatures are the same during emittance and absorptance tests, subtracting equation (A7) from equation (A9) results in

$$\alpha_S AH + P' = P \qquad (A10)$$

$$\alpha_S = \frac{P - P'}{AH} \qquad (A11)$$

Hence, emittance and absorptance are determined by using measurements of temperature, area, power, and solar simulator irradiance.

CALIBRATION OF TOTAL IRRADIANCE OF SIMULATOR

The total irradiance of the solar simulator is measured by two methods. One method utilizes a commercial narrow-angle pyrheliometer, and the other method utilizes a surface whose normal absorptance characteristic is that of a blackbody. It should be emphasized that these methods of measurement determine total irradiance without regard to spectral distribution.

The pyrheliometer uses a thermopile as the sensing element. During measurement of the total irradiance, the pyrheliometer replaces the test specimen mounting assembly and is positioned so that the thermopile is located in the plane of the test specimen with the chamber at atmospheric pressure. Therefore, the total irradiance of the simulator is measured under optical conditions identical to those that exist during absorptance measurements. The pyrheliometer is calibrated against an angstrom compensation pyrheliometer at the Lewis Research Center.

A second method of measuring the total irradiance utilizes a blackbody normal absorptance surface that replaces the test specimen, as described in the section MEASURING TECHNIQUE. An absorptance of 1 is assumed for the surface; hence the total irradiance can be found by using the absorptance measuring technique. The surface consists of a series of parallel notches formed by stacking razor blade edges side by side. Use of a similar reference surface is described in reference 15. A cutaway drawing of the reference surface is shown in figure 12.
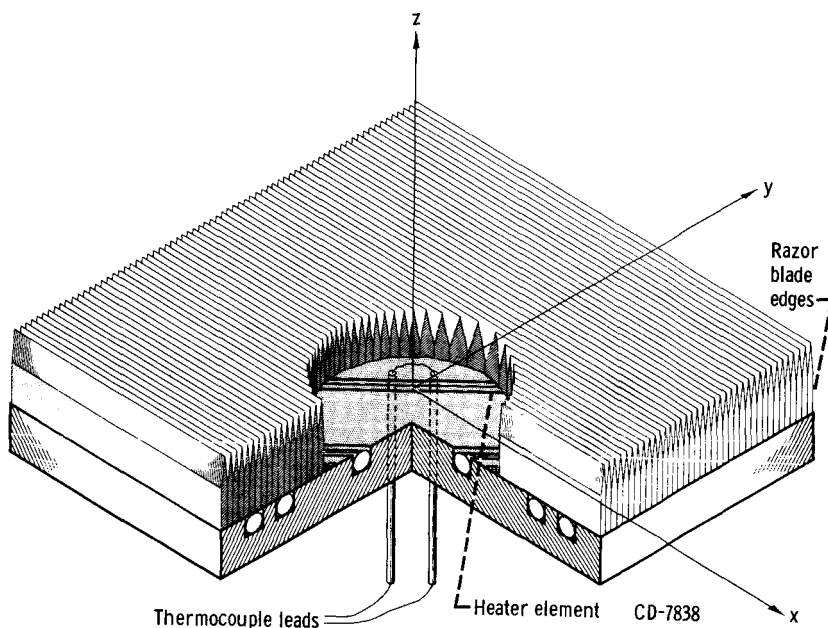

Figure 12. - Reference surface.

An analysis of the notch configuration of the surface indicates a normal solar absorptance greater than 0.99. This analysis is predicted on the assumptions of specular reflection by the notch surfaces and perfectly sharp blade edges. The assumption of specular reflection has been validated by measuring the surface finish of the blades, which was found to be within 4 microinches.

Measurements have shown that the absorptance is independent of the angle of inclination from the normal up to

30°. The angle of inclination is generated by rotating the reference about an axis parallel to the razor blade edges (x-axis in fig. 12). These measurements have also shown that the hemispherical total emittance of the surface is 0.78.

During construction, it was found that the boundary of the reference surface was irregular, and hence the area of the reference surface was not well known. To assure that a known area of reference surface is radiated by the simulator, a temperature-controlled stop is placed directly in front of the razor blades. Since the boundary of the stop is regular and well defined, a known cross-sectional area of the collimated solar beam is incident on the reference. The stop is water cooled to maintain it at the same temperature before and after the simulator is turned on. The two methods of measuring the simulator irradiance agree within 2 percent.

REFERENCES

1. Stockman, Norbert O., and Kramer, John L.: Effect of Variable Thermal Properties on One-Dimensional Heat Transfer in Radiating Fins. NASA TN D-1878, 1963.

2. Nyland, T. W.: Apparatus for the Measurement of Hemispherical Emittance and Solar Absorptance from 270° to 650° K. NASA SP-31, 1963, pp. 393-401.

3. Curtis, H. B.: Measurement of Hemispherical Total Emittance and Normal Solar Absorptance of Selected Materials in the Temperature Range 280° to 600° K. Paper 64-256, AIAA, 1964.

4. Campbell, D. A., and Schulte, H. A.: Measurement of Emissivity at Low Temperatures. Tech. Rep. MT-R2J, Chrysler Corp., Nov. 20, 1957.

5. Butler, C. P.: Solar Absorptance and Emittance of Real Surfaces at High Temperatures. Pt. I. Polished Metals. Research and Development Technical Report. TR-483, Naval Radiological Defense Lab., Dec. 2, 1960.

6. Gordon, G. D.: Measurement of Ratio of Absorptivity of Sunlight to Thermal Emissivity. Rev. Sci. Instr., vol. 31, no. 11, Nov. 1960, pp. 1204-1208.

7. Anon: Measurement of Spectral and Total Emittance of Materials and Surfaces Under Simulated Space Conditions. Rep. PWA-1863, Pratt and Whitney Aircraft, 1960.

8. Anon: IGY Construction Manual. Pt. VI. Radiation Instruments and Measurements. Pergamon Press, 1961.

9. Rachal, L. H.: Fast Response, Low Inertia Vacuum Furnace. Rev. Sci. Instr., vol. 32, no. 8, Aug. 1961, pp. 941-942.

10. Uguccini, Orlando W., and Pollack, John L.: A Carbon-Arc Solar Simulator. Paper 62-WA-241, ASME, 1962.

11. Johnson, Francis S.: The Solar Constant. Jour. Meteorology, vol. 11, no. 6, Dec. 1954, pp. 431-439.

12. Nelson, K. E., and Bevans, J. T.: Errors of the Calorimetric Method of Total Emittance Measurement. NASA SP-31, 1963, pp. 55-65.

13. Askwyth, W. H., and Hayes, R. J.: Determination of the Emissivity of Materials. PWA-2128, Quarterly Prog. Rep. July 1-Sept. 30, 1962, Pratt and Whitney Aircraft, 1962.

14. Brock, C. L., and Ernst, W. A.: Solar Reflective Finish for Space Applications. Rep. AA-3276, Westinghouse Electric Corp., Dec. 1962.

15. Neel, Carr B.: Measurement of Thermal Radiation Characteristics of Temperature-Control Surfaces During Flight in Space. Paper Presented at Ninth Nat. ISA Aerospace Instru. Symposium, San Francisco (Calif.), May 6-8, 1963.